

# Homework 6

ME 7751 Fall 2021

Christopher Bogaev



Mechanical Engineering  
Georgia Institute of Technology  
November 29, 2021

# 1 Program

## Included Files

ME7751\_HW6\_Bogaev\_Christopher.pdf  
ME7751\_HW6\_Problem1\_2.m  
ME7751\_HW6\_Problem1\_3.m  
ME7751\_HW6\_Problem1\_4.m  
ME7751\_HW6\_Problem1\_5.m  
ME7751\_HW6\_Problem1\_6.m

## Directions

Run ME7751\_HW6\_Problem1\_2.m to compute and generate the graphics for Problem 1.2. Adjustments to the spacial domain, time discretization, and spacial discretization can be made in lines 4 - 19.

Run ME7751\_HW6\_Problem1\_3.m to compute and generate the graphics for Problem 1.3. Adjustments to the spacial domain, time discretization, and spacial discretization can be made in lines 4 - 19.

Run ME7751\_HW6\_Problem1\_4.m to compute and generate the graphics for Problem 1.4. Adjustments to the spacial domain, time discretization, and spacial discretization can be made in lines 4 - 19.

Run ME7751\_HW6\_Problem1\_5.m to compute and generate the graphics for Problem 1.5. Adjustments to the spacial domain, time discretization, and spacial discretization can be made in lines 4 - 19.

Run ME7751\_HW6\_Problem1\_6.m to compute and generate the graphics for Problem 1.5. Adjustments to the spacial domain, time discretization, and spacial discretization can be made in lines 4 - 34.

## 2 Results and Discussion

### Problem 1

The two-dimensional cavity of Figure 1 is filled with an incompressible Newtonian fluid. The fluid is driven by the lid moving with a constant velocity  $U$ . This problem is widely used as a benchmark to validate CFD models due to its simple geometry but nontrivial flow solution.

Numerically solve the cavity flow of Figure 1 using the Lattice Boltzmann Method (LBM) with the D2Q9 lattice and BGK collision operator.

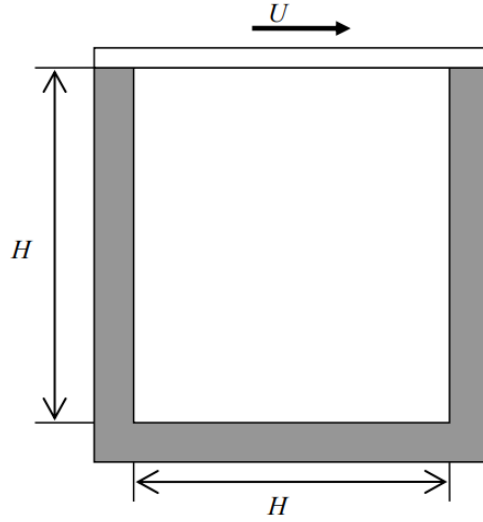


Figure 1: Two-Dimensional Cavity

## Problem 1.1

Traditionally, a quantitative study of fluids relies on either a continuum (macroscopic) or atomistic (microscopic) description. However, an intermediate (mesoscopic) level of description is possible wherein fluids are represented in terms of the probability (density)  $f(r, v, t)$  of finding a given particle at a given position in space,  $r$  and time  $t$ , with a given velocity  $v$  [5]. This intermediate description of fluids is possible with kinetic theory.

In the Boltzmann transport equation (1), the left hand side  $\partial f / \partial t + c \cdot \nabla f$  describes particle streaming and the right hand side  $\Omega$  describes inter-particle collisions.

$$\frac{\partial f}{\partial t} + c \cdot \nabla f = \Omega \quad (1)$$

The Bhatnagar, Gross and Krook (BGK) collision model is used to model the inter-particle collisions  $\Omega$  where  $f^{eq}$  is the Maxwell-Boltzmann equilibrium distribution function.

$$\Omega = \omega(f^{eq} - f) = \frac{1}{\tau}(f^{eq} - f) \quad (2)$$

The streaming and collision steps are performed on the D2Q9 lattice model of Figure 2 wherein the collision step is described in (3) and the streaming step is described in (4) for  $k = 1, 2, \dots, 8$  streaming directions.

$$f_k(x, y, t + \Delta t) = f_k(x, y, t)[1 - \omega] + \omega f_k^{eq}(x, y, t) \quad (3)$$

$$f_k(x + \Delta x, y + \Delta y, t + \Delta t) = f_k(x, y, t + \Delta t) \quad (4)$$

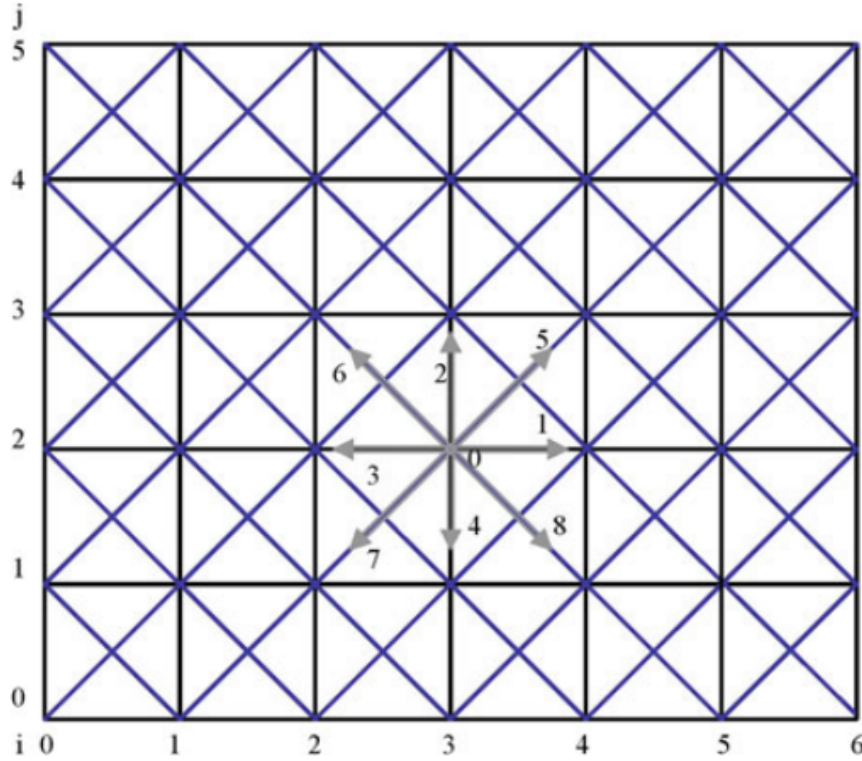


Figure 2: D2Q9 Lattice Model [5]

The bounce back method of Figure 3 is used to model solid stationary or moving boundary condition, nonslip condition, or flow-over obstacles [5]. This method ensures conservation of mass and momentum at the boundaries by extending the streaming process into the wall. In the configuration of Figure 3,  $f_5 = f_7$ ,  $f_2 = f_4$  and  $f_6 = f_8$ , where  $f_7$ ,  $f_4$  and  $f_8$  are known from the prior streaming process (3).

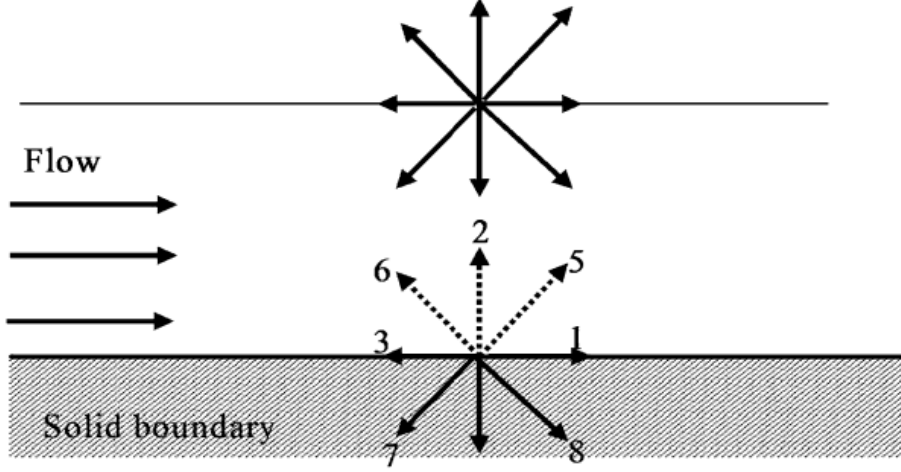


Figure 3: Bounce Back Scheme [5]

The relations between the mesoscopic and the macroscopic quantities for fluid density  $\rho$  and fluid velocity  $u$  are given by (5) and (6) respectively.

$$\rho(r, t) = \int m f(r, c, t) dc \quad (5)$$

$$\rho(r, t) u(r, t) = \int m c f(r, c, t) dc \quad (6)$$

## Problem 1.2

In the square cavity of Figure 1, the Reynolds number, defined by  $Re = UH/\nu$  characterizes the flow patterns. The steady state solutions were computed for both  $Re = 100$ ,  $Re = 400$ , and  $Re = 1000$ . The residual between successive velocity field computations was used as the halting criteria for steady state.

Streamlines were plotted for both  $Re = 100$ ,  $Re = 400$ , and  $Re = 1000$  in Figures 4, 5, and 6 respectively. Additionally, for both  $Re = 100$  and  $Re = 400$ , the x component of velocity was plotted along the vertical centerline in Figure 7 and compared against those found in literature [4]. Similarly, the y component of velocity was plotted along the horizontal centerline in Figure 8 and compared against those found in literature [4]. Excellent agreement was found between the results from the Lattice Boltzmann method and those found in literature [4].

### Solving 2D Steady State Navier Stokes using Lattice Boltzmann

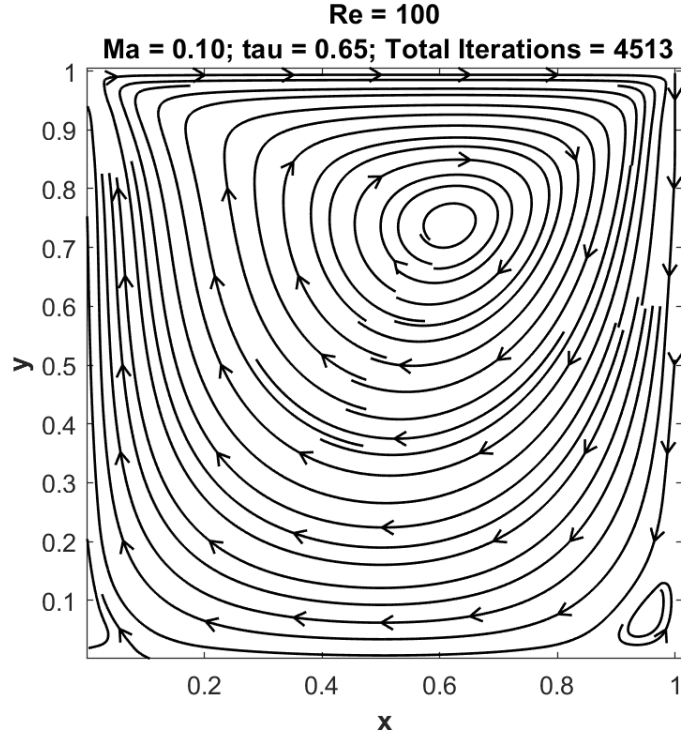


Figure 4: 2D Steady State Solution for  $Re = 100$

**Solving 2D Steady State Navier Stokes using Lattice Boltzmann**

**Re = 400**

**Ma = 0.10; tau = 0.54; Total Iterations = 9292**

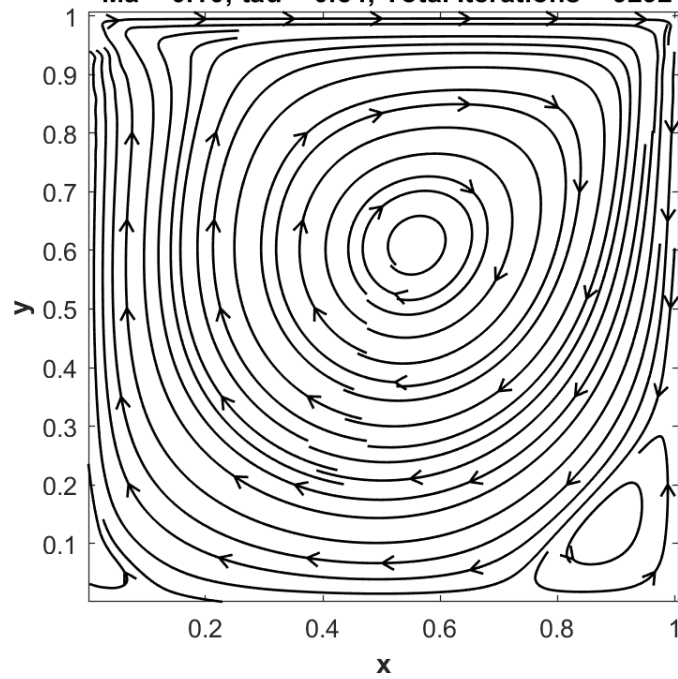


Figure 5: 2D Steady State Solution for Re = 400

**Solving 2D Steady State Navier Stokes using Lattice Boltzmann**

**Re = 1000**

**Ma = 0.10; tau = 0.52; Total Iterations = 14077**

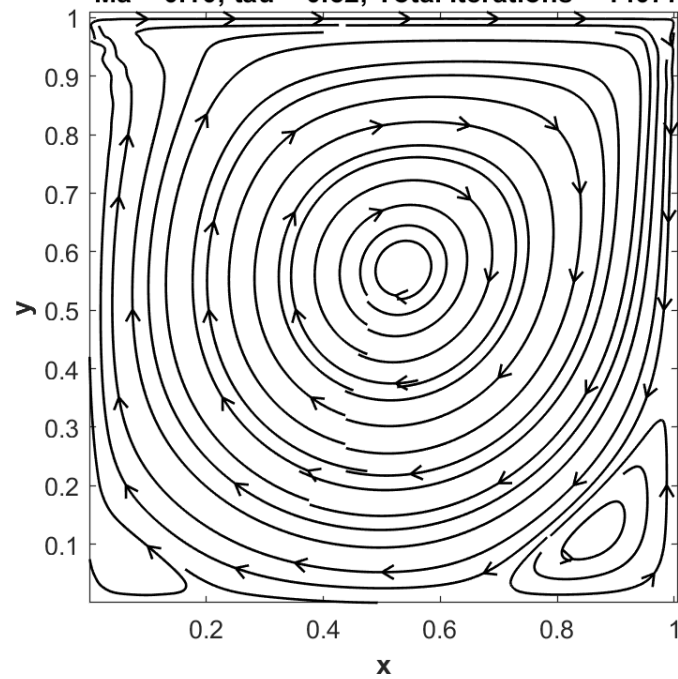


Figure 6: 2D Steady State Solution for Re = 1000

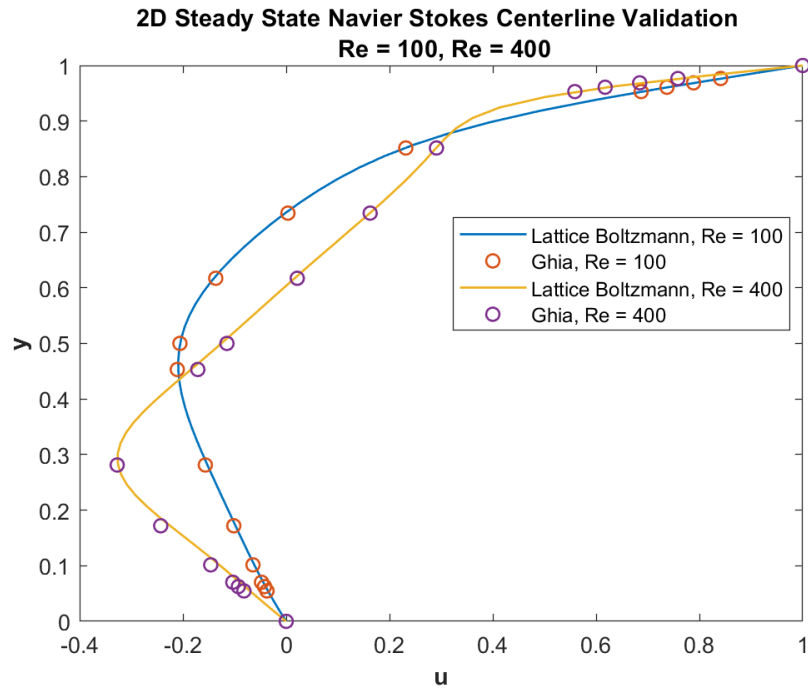


Figure 7: 2D Steady State U-Velocity Centerline Validation

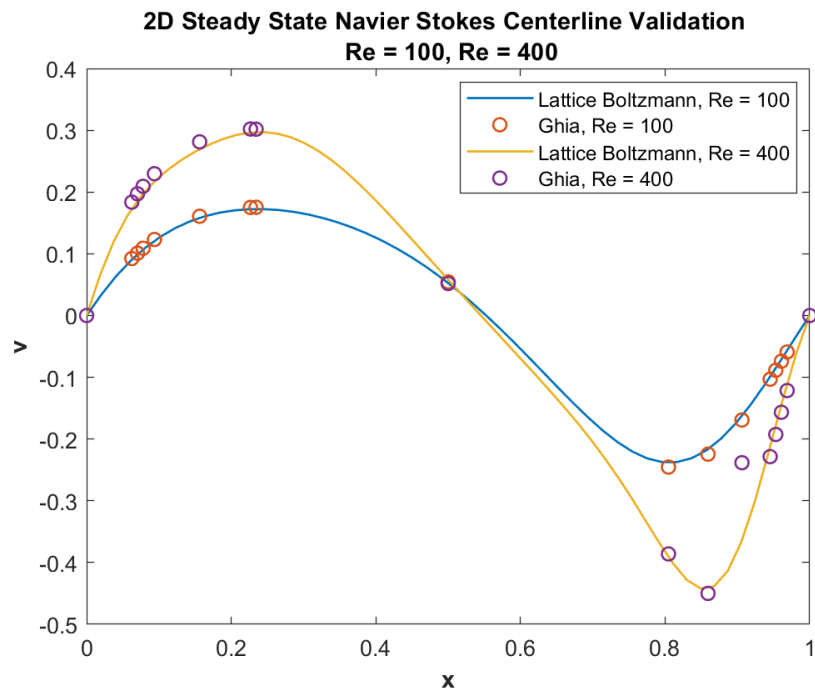


Figure 8: 2D Steady State V-Velocity Centerline Validation



### Problem 1.3

The two centerline  $u$  and  $v$  velocity profiles, for  $Re = 100$  and  $Re = 400$ , are qualitatively shown to converge to the literature values [4] in Figures 9 and 10 for  $Ma = 0.2, 0.1, 0.05$ . Excellent agreement was found between the results from the projection method and those found in literature [4] for  $Ma \leq 0.05$  and  $\tau \geq 0.55$ .

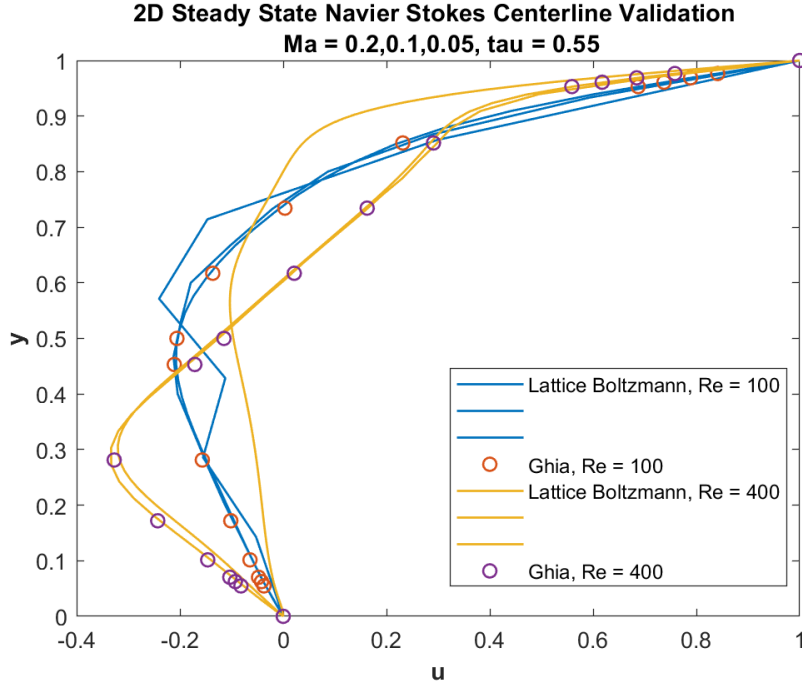


Figure 9: 2D Steady State U-Velocity Centerline Validation

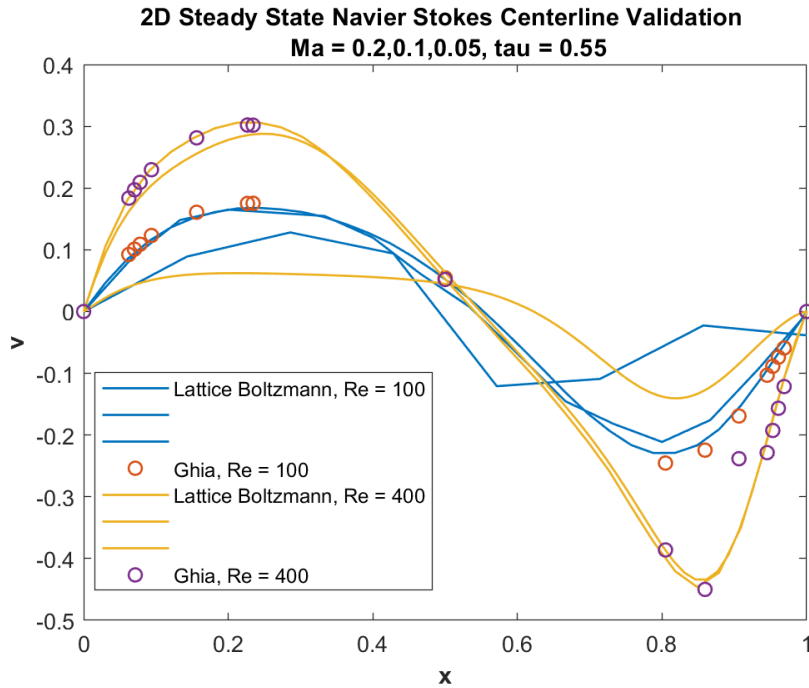


Figure 10: 2D Steady State V-Velocity Centerline Validation

## Problem 1.4

The spacial convergence rate of the Lattice Boltzmann method was numerically computed for  $Ma = 0.2, 0.1, 0.05$ ,  $\tau = 0.55$  and  $Re = 100$  and  $Re = 400$  in Figure 11. The spacial convergence rate was computed by taking the L2 norm of the  $u$  and  $v$  centerline velocities from the method with respect to those found in literature [4]. The theoretical spacial convergence rate was determined to be  $\mathcal{O}(Ma^2)$  matching the numerical spacial convergence rate in Figure 9.

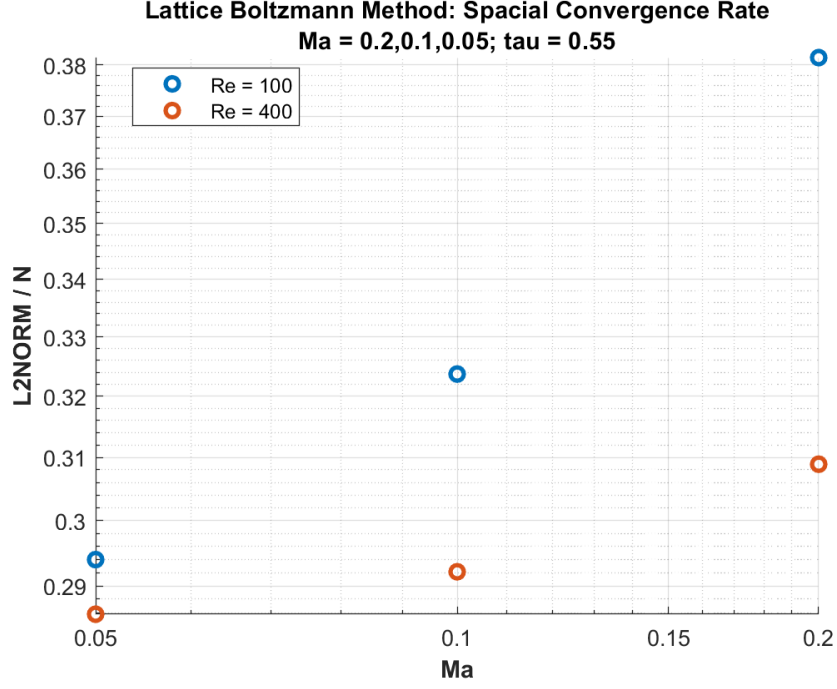


Figure 11: 2D Steady State Spacial Convergence Rate

## Problem 1.5

The spacial convergence rate of the Lattice Boltzmann method was used as an indicator for method stability and was numerically computed for  $Ma = 0.2, 0.1$ ,  $\tau = 0.51, 0.55, 0.60, 0.65$  and  $Re = 100$  in Figure 12. Comparing the results to the stability criteria, the method is stable for  $Ma \leq 0.2$  and  $\tau > 0.5$  thus matching the theoretical stability criteria.

The physical Reynolds number must match the lattice Reynolds number, as shown in (7), for accurate results. However, the lattice Reynolds number is influenced by the lattice Mach number  $Ma$ , the lattice speed of sound  $c_s$ , the grid size  $N$ , the grid step  $\Delta x$ , the lattice time step  $\Delta t$ , and the relaxation time  $\tau$ . Additionally, the lattice kinematic viscosity  $\alpha$ , expressed in (8), must be sufficiently large for method stability, limiting the stable values of  $\tau$ . To match the lattice Reynolds number at high physical Reynolds number, the required grid size becomes large, increasing computational complexity and impacting the feasible range of Reynolds numbers.

$$Re = \frac{UH}{\nu} = \frac{Ma c_s \Delta x N_x}{\alpha} \quad (7)$$

$$\alpha = \frac{\Delta x^2}{3\Delta t}(\tau - 0.5) \quad (8)$$

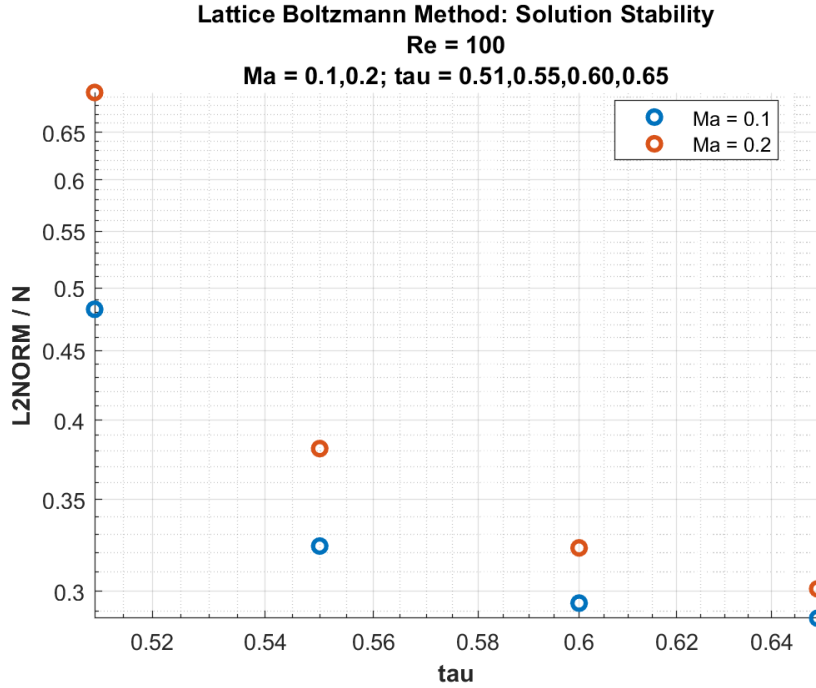


Figure 12: 2D Steady State Solution Stability

## Problem 1.6

For both  $Re = 100$  and  $Re = 400$ , the  $x$  and  $y$  components of velocity were plotted along the vertical centerline in Figures 13 and 14 and compared against those obtained from the artificial compressibility method, projection method and those found in literature [4]. Excellent agreement was found between the results from the projection method, the artificial compressibility method, the Lattice Boltzmann method and those found in literature [4].

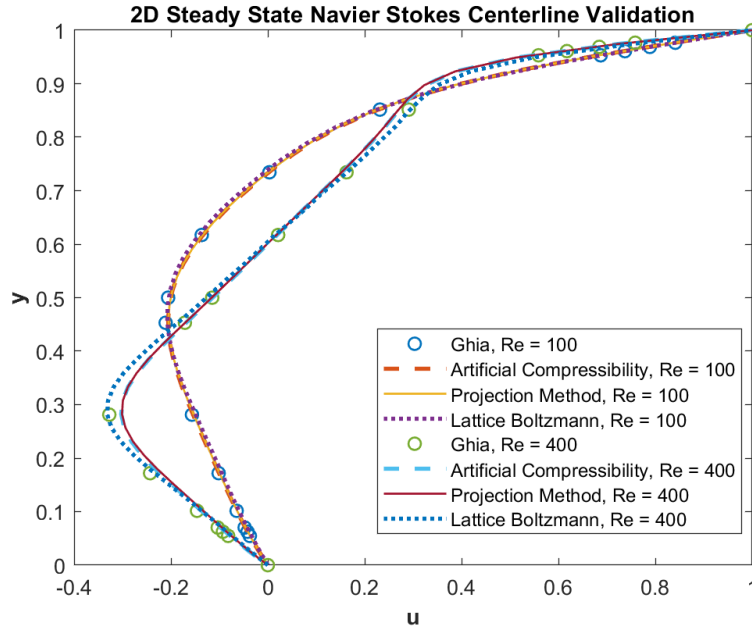


Figure 13: 2D Steady State U-Velocity Centerline Comparison

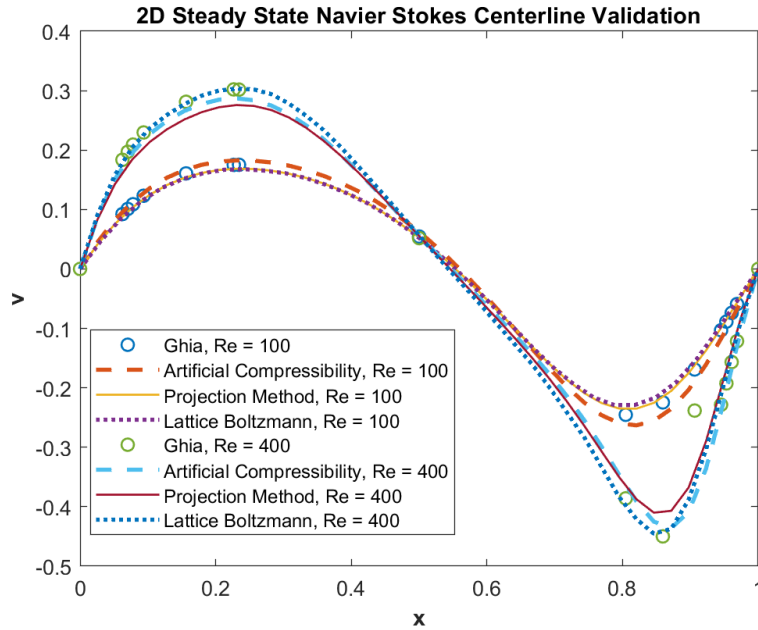


Figure 14: 2D Steady State V-Velocity Centerline Comparison

## References

- [1] J. Ferziger, and M. Perić. *Computational Methods for Fluid Dynamics*. Springer, Berlin, 2nd edition, (1999)
- [2] D. Anderson, J. Tannehill, R. Pletcher *Computational fluid mechanics and heat transfer*. McGraw-Hill, New York, (1984)
- [3] H. Versteeg, W. Malalasekera *An introduction to computational fluid dynamics : the finite volume method*. Pearson Education Ltd., New York, (2007)
- [4] Ghia, U. K. N. G., Kirti N. Ghia, and C. T. Shin. *High-Re solutions for incompressible flow using the Navier-Stokes equations and a multigrid method*. Journal of computational physics 48.3 (1982): 387-411.
- [5] A. A. Mohamad *Lattice Boltzmann method - Fundamentals and engineering applications with computer codes*. Springer, London, (2011)